Chemical Papers (2025) 79:4735–4751
https://doi.org/10.1007/s11696-025-04096-3

ORIGINAL PAPER

Synthesis of thiophene-based imine and phosphoazometine compounds: in vitro antiproliferative, antimicrobial, antioxidant, carbonic anhydrase I and II enzyme inhibition evaluations and molecular docking study

Kubra Ozturk[1] · Muhammet Saban Tanyildizi[2] · Harun Ciftci[3] · Ozlem Gundogdu Aytac[4]

Received: 16 October 2024 / Accepted: 27 April 2025 / Published online: 27 May 2025

Abstract

New thiophene-based imine ((E)-N,N-dimethyl-4-((thiophen-2-yl-methylene)amino)aniline) (**Y6**), amine (N1,N1-dimethyl-N4-(thiophen-2)-ylmethyl)benzene-1,4-diamine) (**Y6a**), and phosphoacomethine (diphenyl (((4-(dimethylamino)phenyl) amino)(thiophen-2-yl)methyl)phosphate) (**Y6b**) compounds were synthesized, and their structures were thoroughly analyzed. The synthesized compounds were determined to have antioxidant effects and strong inhibitory effects against human carbonic anhydrases I and II (hCA I and hCA II) isoforms. All compounds exhibited significant antioxidant properties, with compound **Y6a** showing an IC_{50} value of 5.13 µg/mL, which was significantly lower than the IC_{50} of ascorbic acid (17.55 µg/mL). The compounds also demonstrated potent inhibitory effects against hCA I and hCA II isoenzymes, with IC_{50} values of 1.96 µM (**Y6**), 8.25 µM (**Y6a**), and 0.46 µM (**Y6b**) for hCA I, and 1.89 µM (**Y6**), 0.56 µM (**Y6a**), and 1.02 µM (**Y6b**) for hCA II. In addition to the experimental findings, molecular docking studies of the synthesized compounds were performed. Antimicrobial tests of the synthesized compounds were performed, and it was determined that they have antibacterial activity against bacterial strains. Additionally, all three compounds exhibited promising antiproliferative activity in the MCF-7 breast cancer cell line, with IC_{50} values of 56.58 µM (**Y6**), 51.30 µM (**Y6a**), and 40.01 µM (**Y6b**). Notably, the IC_{50} value of Y6b (40.01 µM) was found to be comparable to that of cisplatin, one of the effective chemotherapy drugs, and has the potential to be a drug or drug precursor.

✉ Kubra Ozturk
kubra.ozturk@ahievran.edu.tr

Muhammet Saban Tanyildizi
mtanyildizi@firat.edu.tr

Harun Ciftci
harunciftci@yahoo.com

Ozlem Gundogdu Aytac
ogundogdu@ahievran.edu.tr

[1] Department of Genetics and Bioengineering, Faculty of Engineering and Architecture, Kırşehir Ahi Evran University, Kırşehir, Türkiye

[2] Department of Bioengineering, Faculty of Engineering, Fırat University, Elazığ, Türkiye

[3] Department of Medical Biochemistry, Faculty of Medicine, Kirşehir Ahi Evran University, Kırşehir, Türkiye

[4] Department of Food Technology, Kaman Technical and Vocational School, Kirşehir Ahi Evran University, Kırşehir, Türkiye

Graphical abstract

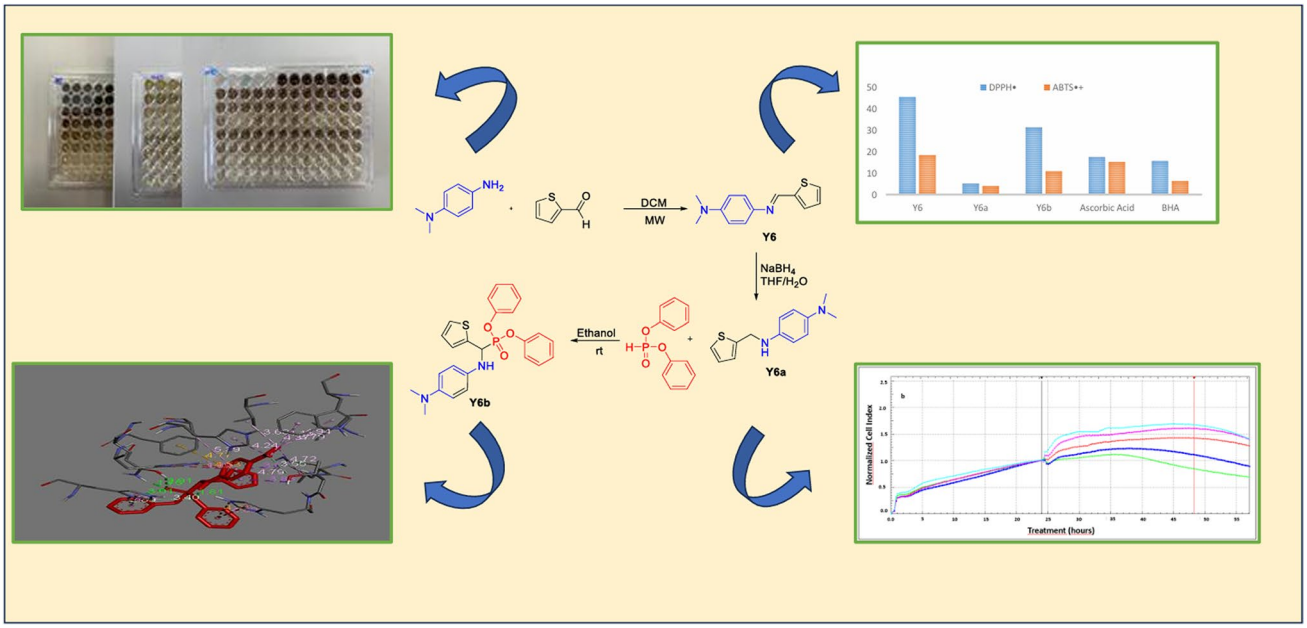

Keywords Phosphanate compound · Antioxidant · Antimicrobial · MCF-7 cells · Carbonic anhydrase

Introduction

In recent years, cancer has become one of the most important public health problems worldwide. Rapid population growth and increased exposure to etiological factors with aging are leading to an increase in cancer incidence. This indicates that a large increase in the burden of cancer is projected in the future, with cancer-related deaths expected to reach 20.3 million in 2030 (Khan 2019). Breast cancer, one of the most common types of cancer, is responsible for 25% of cancer cases in women and 15% of cancer-related deaths (Shams-White et al. 2020). Despite extensive research and investment in the field of cancer, the management, diagnosis, and treatment of human malignancies remains a major challenge. Endeavors have been focused on chemotherapy as a primary chemotherapeutic strategy, although its effectiveness is hindered by notable limitations stemming from the creation of free radicals and reactive oxidant species (ROS), consequently leading to severe side effects (Tuli et al. 2023). In physiological contexts, a modest ROS level assumes a protective role within cells. However, the excessive accumulation of ROS within cellular environments can trigger oxidative stress, culminating in detrimental consequences such as genomic instability. ROS interacts with membrane lipids, nucleic acids, proteins, enzymes and other smaller molecules, thereby causing cellular damage (Aggarwal et al. 2019). Considering the context above, the focus has shifted toward the development of pharmaceutical agents that exhibit a dual capacity encompassing both antioxidant and anticancer effects. This approach aims to counteract the presence of free radicals and ROS, thereby mitigating and preventing the adverse effects associated with chemotherapy, while concurrently targeting and eliminating tumor cells (Cauli 2021).

A previous study has indicated that molecules possessing antioxidant properties can act as inhibitors of carbonic anhydrase (CA) enzymes (Huyut et al. 2016). CA enzymes are crucial zinc metalloenzymes present in all living organisms. They catalyze the reversible conversion of CO_2 and H_2O into HCO_3^- and H^+ ions. Within the human body, a total of 15 distinct CA isoforms have been identified. These isoforms exhibit variations in terms of molecular characteristics, subcellular localization, and distribution across different tissues. CA isoforms play pivotal roles in numerous physiological processes including respiration, pH regulation, sodium (Na^+) retention, calcification, bone resorption, signal transduction, electrolyte secretion, gluconeogenesis, ureagenesis, and lipogenesis. Their diverse involvement in metabolic functions has made CA enzymes valuable targets for therapeutic interventions across various medical conditions such as glaucoma and epileptic seizures, altitude sickness, and more recently, their potential applications extend to the treatment of cancer, obesity, and pain management (Durmaz et al. 2022; Haapasalo et al. 2020). Researchers have extensively

studied and recognized the cytosolic CA I and II isoforms. CA I is prominently expressed in red blood cells and the gastrointestinal tract, whereas CA II is present in all tissues (Yigit et al. 2022). The potential of CA I and II isoforms as a tumor-associated isoform have not been extensively investigated. However, according to the Cancer Genome Atlas (TCGA) database, moderate to high levels of CA I mRNA have been detected in patients with acute myeloid leukemia, colorectal cancer, and renal carcinoma based on RNA sequencing (Uhlen et al. 2017). A recent study has shown that CA I contributes to breast microcalcification, tumorigenesis and migration in breast cancer. A reported that CA I expression is increased in breast cancer, induces abnormal cell calcification, apoptosis, and migration, and may be a potential oncogene (Mboge et al. 2018; Zheng et al. 2015). CA II has been found in different brain tumors, with the most malignant type exhibiting the strongest expression. In addition, this isoform has been associated with poor prognosis in patients suffering from these tumor types (Haapasalo et al. 2020). Furthermore, research has indicated that the inhibition of the CA II isoform contributes to a further reduction in angiogenesis, achieved through its capability to suppress the signaling of vascular endothelial growth factor receptors (Annan et al. 2019).

Cancer treatment methods such as chemotherapy, radiotherapy, and immunotherapy have a negative effect on the patient's immune system. This makes the body more vulnerable to microbial infections. In this context, the development of small molecules as anticancer and antimicrobial agents is of great importance and numerous drugs (Linezolid, GAR-936, Daptomycin, Oritavancin, etc.) are already available for this purpose (Roy and Trinchieri 2017). However, the problem of multidrug resistance is widespread in the fight against both cancer and microbial infections. Therefore, it is necessary to synthesize and develop new precursor molecules with different mechanisms of action that can overcome the problem of multidrug resistance.

In this context, many pharmacologically effective Schiff base compounds are used. Schiff bases are compounds formed by the nucleophilic addition reaction of carbonyl compounds with amines and contain a carbon–nitrogen double bond (–CH=N–) (Puchtler and Meloan 1981). These compounds, also known as imines, are an important class of ligands due to their structural diversity, ability to form stable complexes, ease of preparation, biological conversion, and recombination mechanism (Pathania et al. 2019). The use of Schiff base ligands with electron-donating atoms such as S, O, N, and their complexes is quite common in industrial and clinical research (Kundu et al. 2016; Pathania et al. 2019). S serves as a vital constituent in the regulation of normal physiological processes. It plays a fundamental role in the composition of amino acids, encompassing cysteine, methionine, taurine, and various other sulfur-containing compounds. Additionally, S is an indispensable component of numerous antioxidant molecules such as glutathione, thioredoxin, and glutaredoxin, contributing significantly to their efficacy in combating oxidative stress (Francioso et al. 2020). Furthermore, several studies show that heterocyclic Schiff bases containing N, O, and S atoms possess a wide range of biological activities such as antimicrobial (Pathania et al. 2019), analgesic (Afridi et al. 2022), antioxidant (Ambika et al. 2019) and enzyme inhibition activities (Buldurun et al. 2019).

Organophosphorus compounds are also an effective group of drugs (Mansoura Ali and El-Gendy 2022). Heterocyclic compounds that incorporate organophosphorus groups play a crucial role in various fields including natural product studies, environmental chemistry, organic chemistry, medicinal chemistry, and pharmacology (Finkbeiner et al. 2020). Some of these compounds are alkylating agents and cross-link DNA (Ullah 2020). Oxazaphosphorines and cyclophosphamides are organophosphorus compounds that constitute an effective class of anticancer drugs (Mansoura Ali and El-Gendy 2022). In addition, phosphorus-containing compounds have been reported to be included in the structure of substances used as CA inhibitors (Winum et al. 2005).

Schiff bases and their derivatives are found in natural, semi-synthetic and synthetic compounds and exhibit a wide range of biological activities (Aguilar-Llanos et al. 2022; Chen et al. 2023; Da Silva et al. 2011; Iwanejko et al. 2021). Figure 1 shows some bioactive imine-based molecules.

In light of this information, thiophene-based imine and phosphoazomethine compounds with high biological activity were synthesized in our study and it was aimed to contribute to the studies in this field by investigating the bioactivities of these compounds. Various analysis methods such as elemental, ^{13}C-NMR, ^{1}H-NMR, and FT-IR spectrophotometry were used for the characterization of the synthesized compounds. For the biological activity tests of the newly synthesized derivatives, antioxidant properties were investigated using $ABTS^{\cdot+}$ and $DPPH^{\cdot}$ scavenging ability assays and inhibitory activities against hCA I and II by esterase activity assays. In addition, in vitro antitumor and antimicrobial properties were investigated using the MCF-7 cell line and various microbial strains.

Materials and methods

Chemicals

All materials were commercially purchased from Sigma-Aldrich and used as received without further purification. The solvents used were of analytical grade and no drying or purification was required. The reactions were performed in a household microwave oven (Vestel MD 20 DB model,

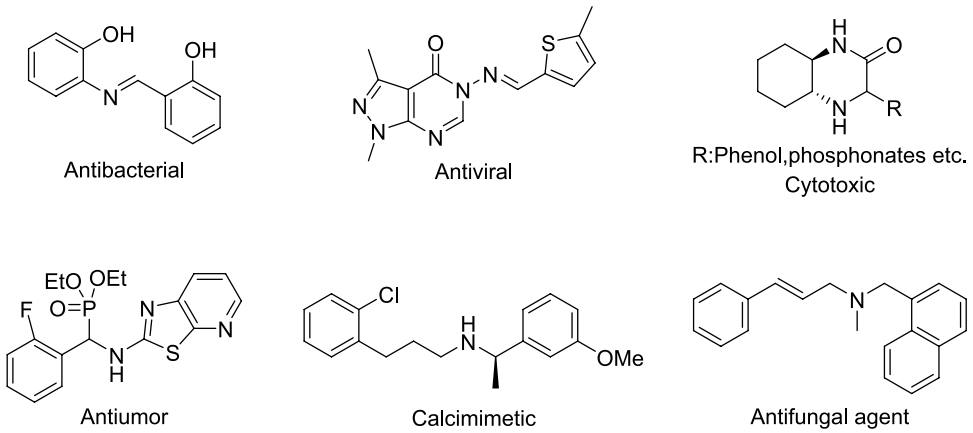

Fig. 1 Different bioactive Schiff base derivatives

230 V–50 Hz, 700 W) and were monitored using thin-layer chromatography (TLC, 60-mesh, Darmstadt, Germany). ^{1}H NMR and ^{13}C NMR spectra were obtained with Varian 400 MHz and Bruker 400 MHz instruments, respectively, using deuterated chloroform ($CDCl_3$) solvent. Elemental analysis results were obtained using a LECO CHNS-932 instrument. Melting points were measured using a Gallenkamp melting point apparatus, and IR spectra were obtained using a Perkin-Elmer Spectrum One FT-IR spectrometer.

Synthesis of N,N-dimethyl-4-((thiophen-2-yl-methylene) amino) aniline (Y6)

Schiff base **Y6** was synthesized by making some modifications to the procedures given in the literature (Ayaz et al. 2022; AYTAÇ 2021). For the synthesis of compound **Y6**, *N,N*-dimethylbenzene-1,4-diamine (1 equiv., 300 mg) and thiophene-2-carboxyaldehyde compound (1 equiv., 247 mg) were dissolved in 1 mL of DCM and exposed to microwave radiation at 900 W for 10 min. left (Scheme 1). The progress of the reaction was monitored by TLC. After the reaction was completed, the solvent was removed in the rotary evaporator and the compound was purified by crystallization in the DCM-Hexane solution system (4:1). It was obtained in 98% yield as a dark green solid. m.p. 132–134 °C. **^{1}H NMR** (400 MHz, $CDCl_3$, δ, ppm): δ 8.64 (s, 1H), 7.47–7.42 (m, 2H), 7.29–7.26 (m, 2H), 7.15–7.12 (m, 1H), 6.77 (d, J = 9.0 Hz, 2H), 3.01 (s, 6H). **^{13}C NMR** (100 MHz, $CDCl_3$, δ, ppm): 149.52, 148.78, 143.77, 140.39, 130.64, 128.99, 127.59, 122.32, 112.84, 40.72. **FT-IR** (KBr, cm^{-1}, ν): Aromatic (CH) 3091, Aliphatic (CH) 2886, 2853, 2803, ν(C = N) 1613. **Elemental analysis** calcd. for $C_{13}H_{14}N_2S$; C, 67.84; H, 6.26; N, 12.21; S, 13.69; found C, 67.79; H, 6.13; N, 12.16; S, 13,92. **HRMS**: (ESI), m/z: Calculated for $[M + H]^+$ $C_{13}H_{14}N_2S$; 231.0878; Found: 231.0950.

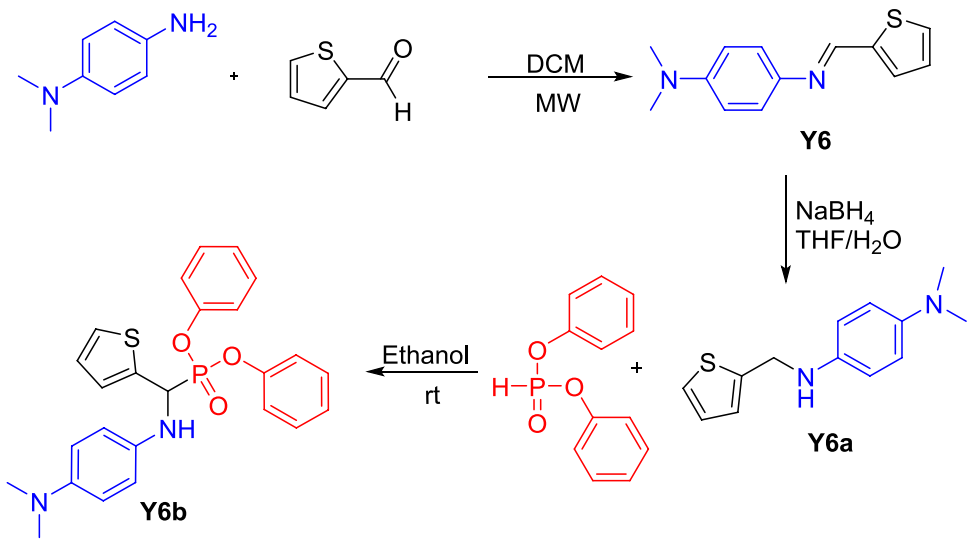

Scheme 1 Synthesis of Schiff base derivatives

Synthesis of N_1,N_1-dimethyl-N4-(thiophen-2-ylmethyl) benzene-1,4-diamine (Y6a)

N_1,N_1-dimethyl-*N*4-(thiophen-2-ylmethyl)benzene-1,4-diamine (**Y6a**) was synthesized by making some modifications to the procedures given in the literature (Ignatovich et al. 2009; Oboňová et al. 2023). After *N,N*-dimethyl-4-((thiophen-2-yl-methylene)amino)aniline (**Y6**) (1 equiv., 350 mg) was dissolved in THF/H_2O (1:1, 20 mL), $NaBH_4$ (8 equiv., 328.50 mg) was added slowly at 0 °C (Scheme 1). The reaction mixture was agitated at room temperature for a duration of 6 h. The progress of the reaction was monitored by TLC and after completion of the reaction the solvent was removed on a rotary evaporator and the compound was purified by crystallization and obtained as a dark green solid in 90% yield. M.p: 59–60 °C. **^{1}H NMR** (400 MHz, $CDCl_3$, δ, ppm): δ 7.12 (dd, J = 5.0, 0.8 Hz, 1H), 6.94–6.86 (m, 2H), 6.66 (d, J = 8.8 Hz, 2H), 6.59 (d, J = 8.8 Hz, 2H), 4.39 (s, 2H), 2.75 (s, 6H). **^{13}C NMR** (100 MHz, $CDCl_3$, δ, ppm): 144.62, 143.60, 140.02, 126.76, 124.81, 124.42, 115.64, 114.87, 44.69, 42.11. **FT-IR** (KBr, cm^{-1}, υ): (NH) 3434. **Elemental analysis** calcd. for $C_{13}H_{16}N_2S$; C, 66.88; H, 7.29; N, 12.04; S, 13.79; found C, 66.98; H, 7.35; N, 12.02; S, 13.76 **HRMS**: (ESI), m/z: Calculated for $[M+H]^+$ $C_{13}H_{16}N_2S$; 232.1034; Found: 233.1070.

Synthesis of diphenyl (((4-(dimethylamino)phenyl) amino) (thiophen-2-yl)meth66.8yl)phosphate (Y6b)

Compound **Y6** (1 equiv., 300 mg) was dissolved in 5 ml of ethanol and diphenylphosphite (1 equiv., 302.40 mg) was added (Scheme 1). The reaction was stirred at room temperature for 2 days and a white solid formed (Rostamizadeh et al. 2011). This solid was filtered through filter paper, washed 3 times with ethanol, and dried. It was obtained in 94% yield without any purification. M.p: 128–129 °C; **^{1}H NMR** (400 MHz, $CDCl_3$, δ, ppm): 7.35–7.26 (m, 6H), 7.17 (ddd, J = 12.6, 7.6, 0.8 Hz, 4H), 7.03 (ddd, J = 11.3, 5.5, 2.7 Hz, 3H), 6.73 (s, 4H), 5.36 (dd, J = 23.7, 7.7 Hz, 1H), 4.38 (brs, 1H), 2.86 (s, 6H). **^{13}C NMR** (100 MHz, $CDCl_3$, δ, ppm): 150.40, 150.30, 145.36, 138.95, 137.42, 129.74, 127.28, 126.89, 125.80, 125.35, 120.77, 120.49, 116.22 (2 C), 115.05 (2 C), 54.13, 41.76. **FT-IR** (KBr, cm^{-1}, ν): 3426(NH), Alifatic (CH) 2853. **Elemental analysis** calcd. for $C_{25}H_{25}N_2O_3PS$; C, 64.51; H, 5.45; N, 6.07; found C, 64.55; H, 5.43; N, 6.04. **HRMS**: (ESI), m/z: Calculated for $[M+H]^+$ $C_{25}H_{25}N_2O_3PS$; 265.1323; Found: 465.1357.

Determination of radical scavenging capabilities

The DPPH scavenging activity of all the synthesized compounds (**Y6, Y6a, Y6b**) was evaluated according to the Blois method, using the following procedure (Blois 1958). Briefly, different concentrations (2–25 µg/mL) of the test compound in 1 mL DMSO were added to 3 mL methanol-DPPH· solution. The samples were incubated for 30 min at room temperature in the dark, and the absorbance values were measured at 517 nm and recorded.

In the ABTS assay method, an aqueous solution of $ABTS^{\cdot+}$ (7.0 mM) was oxidized to its radical cation form ($ABTS^{\cdot+}$) using oxidants such as $K_2S_2O_8$ (2.5 mM) (Re et al. 1999). The resulting $ABTS^{\cdot+}$ solution was then diluted with phosphate buffer (0.1 M, pH 7.4) to give a control absorbance of 0.750 ± 0.025 at 734 nm. Subsequently, 1 mL of $ABTS^{\cdot+}$ solution was mixed with 3 mL of solutions containing compounds (**Y6, Y6a, Y6b**) at different concentrations (2–25 µg/mL). After an incubation period of 30 min, the residual absorbance of $ABTS^{\cdot+}$ was measured at 734 nm. All assays and analyses were performed in triplicate, and results were presented as mean ± standard deviation.

Determination of antibacterial and antifungal activity

The antimicrobial activities of the synthesized molecules were determined by the agar well method using different strains of bacteria and yeast (Berkow et al. 2020). The tested bacterial and yeast strains were obtained from Kırşehir Ahi Evran University Medical Biology Laboratory. In the study, *Klebsiella pneumoniae* (ATCC 10031), *Escherichia coli* (ATCC 25922), *Yersinia pseudotuberculosis* (ATCC 911), *Listeria monocytogenes* (ATCC 43251), *B. subtilis subs. spizizenii* (ATCC 6633), *Staphylococcus aureus* (ATCC 25213), *Staphylococcus aureus BT* (ATCC 25923), *Enterococcus faecalis* (ATCC 29212), *Bacillus cereus* (709 Roma), *Pseudomonas aeruginosa* (ATCC 43288), *Candida tropicalis* (ATCC 13803) and *Candida albicans* (ATCC 60193).

Bacterial strains were inoculated onto MHA (Müller-Hinton Agar) medium and incubated overnight at 37 °C. After streaking inoculation of cell suspensions adjusted to McFarland 0.5 on MHA medium, 4 mm diameter wells were made using a sterile cork borer. Stock solutions of each synthesized compound were prepared at a concentration of 2.5 mg/mL in %5 DMSO. Subsequently, 50 µl of these solutions were added to individual wells and then incubated at 37 °C for 24 h for bacteria or at 25 °C for 48 h for yeasts (MHA for bacteria and PDA media for yeast). The diameters of the inhibition zones formed around the wells due to the activity of each test compound against bacterial and yeast growth were measured using an antibiogram. Ampicillin at a concentration of 1 mg/mL was used as a positive control, while a 5% DMSO solution was used as a negative control. These experiments were performed in triplicate, and the results presented are the mean of three independent experiments.

Determination of minimal inhibition concentrations (MIC)

The minimum inhibitory concentrations (MIC) of the compounds against microorganisms were determined according to NCCLS guidelines (Lewis and James 2022). After the determination of the compounds by the agar well method, the MIC values were determined by the broth microdilution method using 96-well plates. Different concentrations of **Y6, Y6a, Y6b** molecules were prepared in the range of 2500 µg/mL-19.81 µg/mL (2500, 1250, 625, 312.5, 156.25, 78.125, 39.62, 19.81) using YPD broth (Yeast Peptone Dextrose) liquid media for fungi and MHB (Müller–Hinton Broth) liquid media for bacteria. Appropriate media, test compounds, and McFarland 0.5 turbidity suspensions were added to each well of the plate. Plates were incubated at 37 °C for approximately 24 h for bacteria and at 25 °C for 48 h for fungi, and MICs were determined.

Determination of minimal bactericidal concentrations (MBC)

Concentrations at or above the determined MIC values were selected to determine the MBC value. Then, inoculums were taken from the wells containing the concentrations determined to evaluate the bactericidal effects with the help of a core, and line cultures were made on Petri dishes containing medium. After overnight incubation, the lowest concentration without growth was determined as the MBC.

Determination of hCA I and hCA II activity

The activities of hCA I and hCA II isoenzymes were assessed by the esterase activity method, which is based on the hydrolysis of p-nitrophenylacetate, used as a substrate by hCA enzymes, to give p-nitrophenol or p-nitrophenolate (Verpoorte et al. 1967). In the inhibition studies, p-nitrophenylacetate (3 mM) was used as the substrate and the formation of p-nitrophenol from *p*-nitrophenylacetate was followed by measuring the absorbance at 348 nm at a temperature of 25 °C using a spectrophotometer. The enzyme unit was determined using the absorption coefficient of p-nitrophenyl acetate at 348 nm ($\varepsilon = 5.4 \times 10^3\ M^{-1}\ cm^{-1}$). To determine the IC_{50} value, activity measurements were performed using at least five different concentrations of each compound. In the absence of any molecules, the control activity of hCA I and hCA II isoenzymes was considered 100%. The inhibitor concentrations were plotted against the percentage activity of both isoenzymes, and the IC_{50} values for each molecule were calculated using equations derived from the slope. Acetazolamide (AZA) was used as a reference inhibitor for hCA I and hCA II isoenzymes. All assays and analyses were performed in triplicate, and results were presented as mean ± standard deviation.

Molecular docking studies

The molecular structures of the compounds were created using ChemDraw 19.0 and then converted to PDB format using Avogadro. The resulting compounds were then inserted into the active sites of the hCA I and hCA II isozymes. The crystallographic structures of hCA I and hCA II were obtained from the Protein Data Bank server (PDB codes: 6G3V and 3PO6) (Camadan et al. 2022). Ligands and protein molecules were then converted to PDBQT files formats using AutoDock Tools 1.5.7. Protein–ligand complex files were analyzed using Discovery Studio Software.

Anticancer activity studies

Preparation of samples

To prepare the samples, stock solutions were first created in DMSO and then further diluted using Dulbecco's modified Eagle's medium (DMEM). The final concentration of DMSO was below 1% in all assays.

Cell lines and cell culture

MCF-7 breast cancer cell line (ATCC® HTB −22™) was obtained from Department of Medical Biology, Faculty of Medicine, Başkent University.They were grown in RPMI (Roswell Park Memorial Institute) medium containing 10% fetal bovine serum (FBS), 100 U/mL Penicillin, 100 µg/mL Streptomycin and 5% CO_2 at 37 °C under sterile conditions. The medium was changed twice a week.

Cytotoxicity test

The Real-Time Cell Analyzer (RTCA, iCELLigence) device (Roche Applied Science, Basel, Switzerland) was used to visualize the proliferation inhibitory effects of the synthesized compounds on MCF-7 cell lines. iCELLigence system is an advanced cell analysis system that includes microelectronic biosensors and enables real-time and continuous monitoring of the cytotoxic effects of the applied substances on the cell, cell proliferation, and death over a period of time. The cell surface coverage is determined so that the cell index (CI) value is not less than 0.5 and ideally 1 or higher (Türker Şener et al. 2017). A high CI value indicates how high the population of cells growing on the bottom is and how high the spread of cells is. RTCA allows researchers to analyze cell behavior in a cell-based assay without the need for labeling and provides a real-time profile of the

cells. To evaluate the antiproliferative effects of the synthesized compounds, MCF-7 cells were first detached from the flask surface using a trypsin/ethylenediaminetetraacetic acid solution. Following detachment, an equivalent volume of medium was introduced to the cell suspension and mixed gently. This suspension was subsequently partitioned into Falcon tubes and subjected to centrifugation. Meanwhile, 200 µl of the medium was added to each well of the e-Plate, and the e-Plates were placed in the iCELLingence system and background measurements were performed. After the background measurement, cell seeding was performed with 15.000 cells/450 µl in each well. The e-plates were kept at room temperature for 30 min to allow the cells to settle to the bottom. At the end of 30 min, the e-plates were placed back in the system and the experiment was started to measure every 15 min for 96 h. During the exponential growth phase, at the end of approximately 24 h, the e-plates were removed from the system for the addition of substances and the study was stopped. The synthesized substances were added to the wells at different concentrations (25, 50, 75 µM), and the final volume of each well was adjusted to 450 µL with a culture medium. The control group was made up to 450 µL with medium without the addition of any drug, and DMSO was added to the negative control well at a final concentration of 1%. Measurements were made in duplicate.

Results and discussion

The target thiophene-based imine and phosphoazomethine compounds were obtained in excellent yields (90–98%) following the route shown in Scheme 1. The compounds (**Y6, Y6a, Y6b**) were characterized by elemental analysis, IR, ^{13}C NMR and ^{1}H NMR spectra.

In the IR spectra of compounds (**Y6, Y6a, Y6b**), when the specific ν(CN) vibrations for compound **Y6** were examined, C=N imino stretching was observed at 1613 cm^{-1}. However, an important peak belonging to the carbonyl (C=O) group belonging to the aldehyde was observed at 1700 cm^{-1}. The separation between sp^2 and sp^3 C–H stretching modes at 3000 cm^{-1} was clearly seen. These data support the realization of the formation reaction of the targeted compound, and the results obtained are consistent with the literature data (Nasser et al. 2023).

In the ^{1}H NMR spectrum of compounds (**Y6, Y6a, Y6b**), the single peak of an imine proton at 8.64 observed indicates the formation of the Schiff base. Besides the aldehyde groups, other signals related to 2-aminothiophene were observed as expected and the protons belonging to the thiophene ring were observed at 7.47–7.42 and 7.15–7.12 ppm. Another important peak belonging to the structure was the aromatic -CH protons belonging to the benzene ring at 7.44 and 6.77 ppm, and the methyl -CH_3 protons belonging to the dimethyl amino group were observed as singlet at 3.01 ppm. NH-CH_2 methylene protons, which are the characteristic peak of the structure of the reduction compound, are seen as a singlet peak at 4.39 ppm. The presence of this peak is the most important evidence that the double bond is converted into a single bond. The presence of dimethyl amino peaks and aromatic protons was found to be compatible with the structure. The P–CH proton added to the structure was observed at 4.38 ppm, the methyls of the dimethyl amino moiety at 2.86 ppm, and the NH proton at 5.36 ppm. In addition, the total number of aromatic protons is compatible with the structure and the results obtained are consistent with the literature data (Satapathy et al. 2019).

When the ^{13}C NMR spectra of the compounds (**Y6, Y6a, Y6b**) were examined, the aliphatic methyl (-CH_3) carbon was clearly seen at 40.72 ppm, the carbons belonging to the aromatic ring at 112.84 and 122.32 ppm, respectively, the –C=N carbon at 149.52 ppm, the ipso carbon to which the dimethyl amino group is attached at 148.78 ppm. The presence of two aliphatic peaks and the peak at 44.69 ppm, which proves that the –CH=N bond is transformed into -CH_2-NH bond, is the biggest evidence of the transformation of the structure. In addition, aromatic –CH carbons belonging to the benzene ring were observed at 114.87 and 115.64 ppm, respectively. The ipso carbon to which the dimethyl amino group is attached resonated at 144.62. The appearance of the –P–CH carbon peak at 54.13 ppm in compound **Y6b** in addition to the previous compound, clearly indicates the formation of the compound, and the disappearance of the -NH-CH_2 carbon peak at 44.69 ppm in compound **Y6a**, and the presence of aromatic -CH carbons from two extra phenyls are evidence that the structure is formed. Chemical shifts and peak numbers are consistent with the literature (Shanty et al. 2017).

Antioxidant activity

Researchers often prefer in vitro methods for assessing antioxidant activity due to their ease of application and the rapid results they provide (Liu et al. 2021). In this study, $ABTS^{\cdot+}$ and DPPH· scavenging activities were preferred to determine radical scavenging activity.

The synthesized compounds caused a significant change in both the color and absorption spectrum of DPPH·. It was found that the antioxidant activities of the compounds increased parallel to the concentration. IC_{50} values were obtained from % inhibition vs. concentration graphs plotted against concentration. As shown in Table 1, IC_{50} values of **Y6, Y6a,** and **Y6b** compounds were determined as 45.73 ± 3.50, 5.13 ± 0.40 and 31.53 ± 2.00 µg/mL, respectively. When the results were analyzed, it was observed that **the Y6** compound showed the lowest DPPH· scavenging activity, **the Y6a** compound showed the highest DPPH· radical

Table 1 IC_{50} (µg/mL) values for DPPH· and $ABTS^{·+}$ scavenging abilities of **Y6, Y6a** and **Y6b** compounds and standards

Molecules	DPPH·		$ABTS^{·+}$	
	IC_{50} (µg/mL)	R^2	IC_{50} (µg/mL)	R^2
Y6	45.73 ± 3.50	0.9957	18.45 ± 1.25	0.9843
Y6a	5.13 ± 0.40	0.9903	3.98 ± 0.30	0.9895
Y6b	31.53 ± 2.00	0.9890	10.89 ± 0.75	0.9787
Ascorbic Acid	17.55 ± 1.50	0.9604	15.24 ± 1.20	0.9537
BHA	15.75 ± 1.00	0.9780	6.27 ± 0.50	0.9802

scavenging activity, and this value was higher than ascorbic acid and Butylated hydroxyanisole (BHA). As shown in Table 1, the results exhibited compounds (**Y6, Y6a, Y6b**) with high $ABTS^{·+}$ scavenging ability. IC_{50} values of **Y6, Y6a,** and **Y6b** compounds were determined as 18.45 ± 1.25, 3.98 ± 0.30 and 10.89 ± 0.75 µg/ml, respectively. When the results were analyzed, similar to DPPH· scavenging activity, the **Y6** compound showed the lowest $ABTS^{·+}$ scavenging activity, whereas the **Y6a** compound showed the highest $ABTS^{·+}$ radical scavenging activity and this value was higher than ascorbic acid and BHA. The presence of the N–H group in the **Y6a** molecule, as reported by Nguyen et al., provides hydrogen atom to DPPH radicals (Nguyen et al. 2013), which makes the compound itself a radical and increases the total antiradical capacity by reacting with other DPPH· radicals. Vukovic et al. found that amines (IC_{50}: 25.9–138 µM) have higher radical trapping capacity than imines (IC_{50}: 304.1–446.9 µM) (Vukovic et al. 2010). The aromatic ring structures of some commonly used antioxidant substances (e.g. ascorbic acid) facilitate the displacement of unpaired electrons (Marchi et al. 2022). It has been shown in other studies that Schiff bases and their electron-donating groups such as oxygen, sulfur, and nitrogen exhibit important biological activities (Savcı et al. 2022; Venkateswarlu et al. 2018). Tlidjane et al. successfully synthesized four novel α-aminophosphonate compounds incorporating thiophene ring. Their research demonstrated that these compounds exhibit significant antioxidant potential, even at low concentrations ranging from 16.04 to 26.15 µg/mL. Notably, these compounds displayed greater antioxidant activity compared to established standards like Butylated Hydroxytoluene (BHT) and Butylated hydroxyanisole (BHA). They reported that the high activity of the compounds may be due to the presence of nitro group and heterocyclic ring (Tlidjane et al. 2022). In addition to the aromatic ring, the synthesized molecules also contain azomethine and phosphate groups which affect the radical scavenging activity. The compound's low IC_{50} values are indicative of their effective ability to scavenge radicals. These synthesized compounds have demonstrated the potential to be utilized as promising antioxidant agents, effectively scavenging ROS that can cause damage in humans.

Antimicrobial activity

The antimicrobial activity of the synthesized compounds (**Y6, Y6a, Y6b**) was determined against eleven different microorganisms. Inhibition zone diameters, MIC, and MBC results are given in Tables 2 and 3. DMSO was used as a solvent and found to have no antimicrobial activity against any of the tested organisms. Inhibition test results showed that the compounds did not have antifungal activity against *C. albicans* and *C. tropicalis* strains but had antibacterial activity against all bacterial strains used (inhibition zones ranging from 8 to 18 mm). All test compounds showed the highest activity against *P. aeruginosa* (inhibition zone of 14–18 mm) among Gram-negative bacteria. *P. aeruginosa*

Table 2 Zone diameters values of the compounds against the tested microorganisms

Microorganisms	Zone diameters			
	Y6	Y6a	Y6b	Ampicillin
Gram-negative bacteria				
E. coli (ATCC 25922)	8 ± 0.40	–	–	19 ± 0.87
P. aeruginosa (ATCC 43288)	15 ± 0.89	14 ± 0.68	18 ± 1.30	22 ± 1.12
A. baumannii (ATCC 02026)	12 ± 0.63	–	11 ± 0.43	21 ± 0.93
K. pneumoniae (ATCC 10031)	–	11 ± 0.46	11 ± 0.40	21 ± 0.96
Y. pseudotuberculosis (ATCC 911)	–	–	14 ± 0.63	22 ± 1.11
Gram-positive bacteria				
L. monocytogenes (ATCC 43251)	–	-	11 ± 0.40	20 ± 1.07
B. subtilis (ATCC 6633)	–	–	17 ± 1.10	22 ± 1.17
S. aureus (ATCC 25213)	11 ± 0.44	–	9 ± 0.30	19 ± 0.92
S. aureus BT *(ATCC 25923)*	10 ± 0.40	–	12 ± 0.48	20 ± 0.96
E. faecalis (ATCC 29212)	13 ± 0.60	13 ± 0.42	15 ± 0.75	22 ± 1.05
B. cereus (709 Roma)	–	–	13 ± 0.50	21 ± 0.98

Table 3 MIC/MBK values of the compounds against the tested microorganisms

Microorganisms	MIC Values (µg/mL)			MBK Values (µg/mL)		
	Y6	Y6a	Y6b	Y6	Y6a	Y6b
E. coli (ATCC 25922)	–	–	78.13	–	–	312.50
P. aeruginosa (ATCC 43288)	78.13	39.62	78.13	78.13	78.13	156.30
A. baumannii (ATCC 02026)	78.13	–	39.62	312.50	–	–
K. pneumoniae (ATCC 10031)	–	78.13	78.13	–	312.50	312.50
Y. pseudotuberculosis (ATCC 911)	–	–	78.13	-	-	312.50
L. monocytogenes (ATCC 43251)	–	–	78.13	–	–	156.30
B. subtilis (ATCC 6633)	–	–	39.62	–	–	–
S. aureus (ATCC 25213)	78.13	–	39.62	156.30	–	156.30
S. aureus BT *(ATCC 25923)*	78.13	–	78.13	312.50	–	156.30
E. faecalis (ATCC 29212)	78.13	78.13	78.13	312.50	312.50	312.50
B. cereus (709 Roma)	–	–	78.13	–	–	312.50

is a pathogen that causes burn injuries, urinary tract infections, wounds, and corneal ulcers (Spagnolo et al. 2021). All compounds exhibited the highest antibacterial activity against *E. faecalis*, a Gram-positive bacterium (inhibition zone of 13–15 mm). *E. faecalis* is the most frequently isolated Gram-positive bacterium in hospital environments. It is commonly associated with urinary tract infections and endocarditis outbreaks (Ayobami et al. 2020). The results showed that compound **Y6** had similar antibacterial activity against *A. baumannii, S. aureus, S. aureus BT, E. faecalis* bacteria, and MIC values were determined as 78.13 µg/mL. Compound **Y6b** was effective against *E. Coli, P. aeruginosa, A. baumannii, K. pneumoniae, Y. pseudotuberculosis, L. monocytogenes, B. subtilis, S. aureus, S. aureus BT, E. faecalis, B. cereus* strains. MIC values were determined between 39.62 and 78.13 µg/mL. Compound **Y6a** was found to be effective against three bacterial strains (*P. aeruginosa, A. baumannii, E. faecalis*) and MIC values were determined as 39.62, 78.13, and 78.13 µg/mL, respectively. It is thought that the relative differences in the activity of the compounds against different microorganism species may be due to the difference in the ribosomes of microbial cells or the permeability of their cells. In the literature, there are studies supporting our results, showing that compounds containing Schiff base, thiophene, and phosphate group in their structure have antibacterial and antifungal properties (Eleamen et al. 2017; Gholivand et al. 2022; Venkateswarlu et al. 2018).

Carbonic anhydrase inhibition

hCA isoenzymes have been closely associated with many physiological and pathological processes. Therefore, inhibitors of these isoenzymes are of great importance as target molecules in drug design studies. Since existing hCA inhibitors have some side effects and insufficient specificity, new hCA inhibitors need to be discovered (Köksal et al. 2019). In this study, the inhibition effects of new thiophene-based imine and phosphoazomethine (**Y6, Y6a, Y6b**) compounds on hCA I and hCA II activities were investigated.

Inhibition data of hCA I and hCA II isozymes are given in Table 4. IC_{50} values for hCA I were found to be 1.96 ± 0.15, 8.25 ± 0.50, and 0.46 ± 0.05 µM for compounds **Y6, Y6a,** and **Y6b**, respectively. IC_{50} values for hCA II isoenzyme were determined as 21.89 ± 0.12, 0.56 ± 0.05 and 1.02 ± 0.08 µM, respectively. It was observed that all compounds had an inhibitory effect on hCA I and hCA II at micromolar concentrations. When these values were compared with the reference inhibitor AZA, it was observed that **Y6, Y6a,** and **Y6b** molecules had an inhibitory effect close to AZA on hCA I and hCA II activity. Compound **Y6b**, which contains phosphate groups in its structure, showed the strongest inhibitory effect for hCA I, while compound **Y6a** showed a significant inhibitory activity for hCA II. The variance in the inhibition rates of the compounds against hCA I and hCA II isoenzymes can be attributed to the distinct catalytic activities and inhibitor sensitivities exhibited by these hCA isoenzymes. When the literature data were examined, it was observed that Schiff bases have high inhibition properties against important metabolic enzymes such as hCA, AChE, and BChE, which are associated with many diseases (Aytac et al. 2023). In a study by Yiğit et al. (2018), three

Table 4 Inhibition results of **Y6, Y6a** and **Y6b** compounds on hCA I and hCA II isoenzymes

Compounds	hCA I		hCA II	
	IC_{50} (µM)	R^2	IC_{50} (µM)	R^2
Y6	1.96 ± 0.15	0.958	1.89 ± 0.12	0.945
Y6a	8.25 ± 0.50	0.984	0.56 ± 0.05	0.996
Y6b	0.46 ± 0.05	0.922	1.02 ± 0.08	0.977
AZA*	0.54 ± 0.06	0.984	0.28 ± 0.03	0.988

*Acetazolamide (AZA): an inhibitor used as a standard for hCA I and hCA II isoenzymes

series of symmetric Schiff bases and their amine derivatives were tested against AChE, hCA I, and II isoenzymes and reported to show an inhibition effect at nanomolar concentrations (Yiğit et al. 2018). In another study by Gülcin et al. (2020), they synthesized heterocyclic compounds containing nitrogen, phosphorus, selenium, and sulfur and determined that they have an inhibition effect against hCA I in the range of 33.32–60.79 nM and against hCA II in the range of 37.05–66.64 nM (Gülçin et al. 2020). When the studies were examined, it was observed that studies on phosphonates as CA inhibitors were limited. However, there are a few studies showing that compounds containing phosphonate groups are also strong hCA inhibitors (Nocentini et al. 2019; Sobati et al. 2023). Zareei et al. added phosphonate groups to sulfonamide compounds with proven inhibition activity on hCAs. They found that most of the series of sulfonamide-phosphonate hybrid compounds they synthesized had stronger inhibitory activity than the standard inhibitor AZA (Zareei et al. 2023). In agreement with the literature, our results revealed that Schiff base, amine, and phosphoazomethine compounds containing thiophene in their structure have high inhibitory properties against hCA I and hCA II. It is thought that the results obtained may be useful in the synthesis of new hCA isoenzyme inhibitors and in the development of drugs for the treatment of some diseases.

Anticancer activity

To determine the antiproliferative effects of the compounds, 3 different compound doses (25–75 µM), 1% DMSO, and control were studied. The results were compared with the standard cancer drug Cisplatin. Substance addition was performed at approximately 24 h after cell seeding. Approximately 24 h after the addition of the substance, IC_{50} values were calculated by the nonlinear regression using the sigmoidal dose response (variable slope) method. IC_{50} values of **Y6, Y6a,** and **Y6b** compounds were determined as 56.58 ± 5.40, 51.30 ± 4.98, and 43.76 ± 3.57 µM, respectively. From the results obtained, it was observed that the treatment with the **Y6** compound was ineffective at a dose of 25 µM, at 50 µM, the proliferation initially passed to the stationary phase, and then, although some proliferation was observed, it passed to the stationary phase again, but the cells did not pass to the death phase. At 75 µM, it was observed that the cells passed to the death phase after the stationary phase after incubation (Fig. 2a). When the growth curves of cells treated with **Y6a** compound were analyzed, although a classical growth curve with lag, exponential, stationary, and death phases was observed, it showed a decreased exponential phase compared to control cells with low index numbers compared to control cells. At 75 µM concentration, an abrupt decrease in cell proliferation was observed after the exponential phase (Fig. 2b). When **Y6b** was applied at doses of 25 µM and above, the cell index decreased and the cytotoxic effect increased (Fig. 2c). It was observed that all three compounds exhibited good antiproliferative activity in the MCF-7 cell line by causing a decrease in the growth curve rate on CI basis with the increase in concentration compared to control cells. Compounds **Y6** and **Y6a** (56.58 µM, 51.30 µM) exhibited higher IC_{50} values compared to cisplatin (40.01 µM) in the MCF-7 human breast cancer cells, while compound **Y6b** (43.76 µM) showed almost the same IC_{50} value as cisplatin. These differences between the cell growth curves are thought to be due to differences in the mechanisms of action of the active groups. The results obtained show that the addition of phosphonate to thiophene-substituted Schiff bases increases the antiproliferative effect. When recent studies were examined, it was observed that Schiff-based ligands containing thiophene terminals caused growth inhibition in the MCF-7 cell lines (Uluçam et al. 2021), while compounds containing phosphonic acid and phosphonate moieties showed low cytotoxicity against normal cell lines (mouse fibroblasts-BALB/3 T3) and showed a strong antiproliferative effect against leukemia cell line (MV-4–11) (Iwanejko et al. 2020). In the study by Abd Elghany El-Samahy et al. (2023), a series of aminophosphonate derivatives were synthesized by the reaction of imines with dialkyl phosphites by Pudovik reaction. They investigated the cytotoxic activity of the synthesized compounds in the MCF-7 cell line and reported that they showed higher cytotoxicity against the MCF-7 cell line than the reference drug doxorubicin (Abd Elghany El-Samahy et al. 2023). In another recent study, they synthesized a series of compounds containing α-aminophosphonate and Schiff base and reported that they showed an extremely strong inhibitory activity against the MCF-7 cell line with 94.32% and 92.45% inhibition, respectively (Omar M Ali et al. 2022). In another study, it was observed that the addition of an aminophosphonate group to a pharmacophore core increased antitumor activity (Ye et al. 2014). In the literature, there are studies showing the antitumor effect of Schiff base and aminophosphonate derivatives containing thiophene analog supporting our results. Considering all these, it is predicted that the obtained compounds exhibit high activities and may serve as promising antitumor candidates for chemotherapeutic drug studies.

Molecular docking studies

Molecular docking studies were performed to predict the binding conformations and non-covalent interactions between the synthesized ligands and hCA I and hCA II enzymes. Molecular docking calculations were performed using the AutoDock Tools 1.5.7 program. In addition, two-dimensional interaction diagrams and three-dimensional interaction diagrams were visualized with BIOVIA

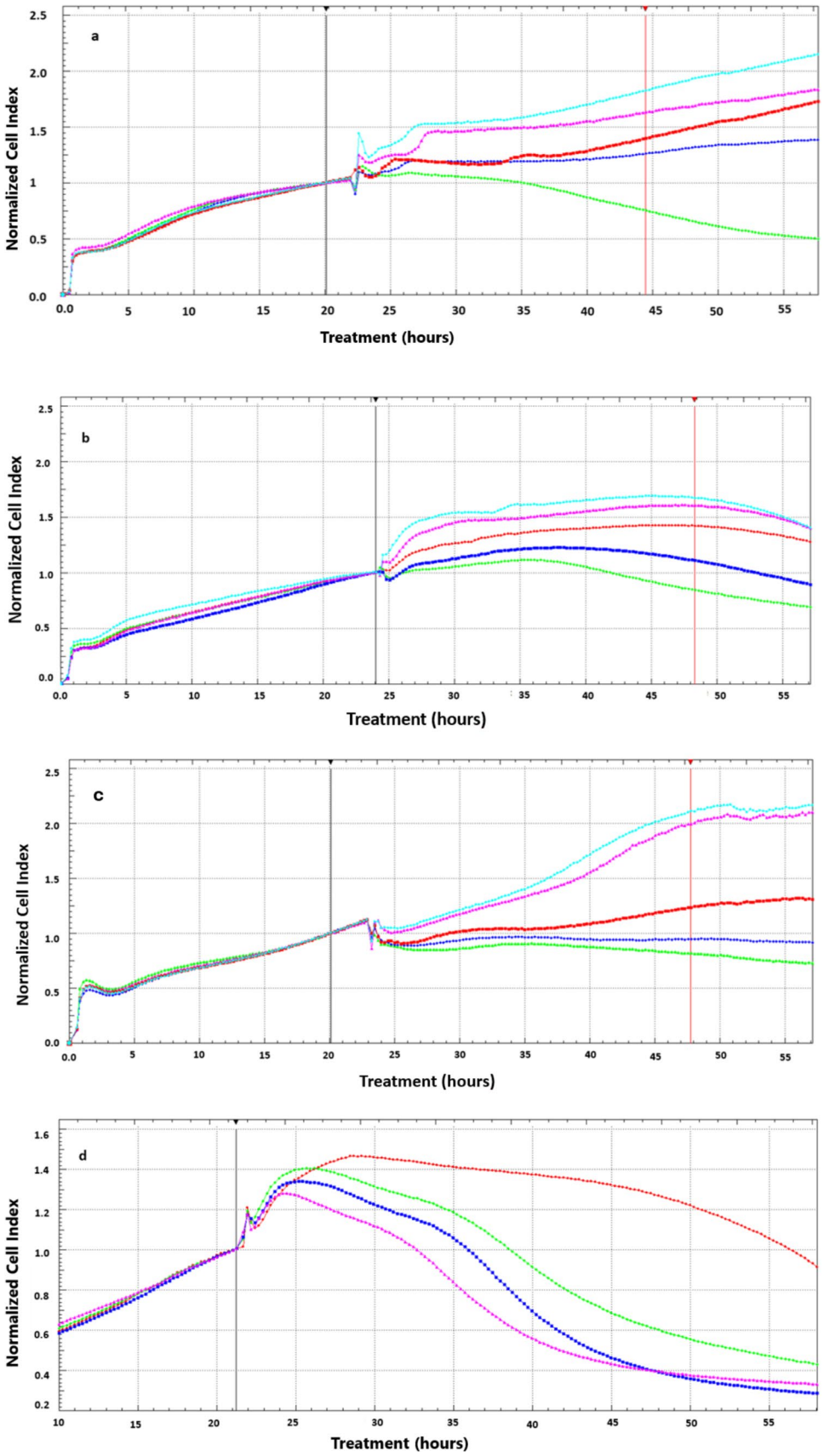

Fig. 2 Effects of compound Y6 (**a**), Y6a (**b**), Y6b (**c**) (Turquoise: Control, Pink: DMSO, Red: 25 uM, Blue: 50 uM, Green: 75 uM) and cisplatin (**d**) (Red: Control, Green: 25 uM, Blue: 50 uM, Pink: 75 uM) on MCF-7 cell proliferation in real time using the iCELLigence cellular analysis system

Discovery Studio software. The crystal structures of the target proteins (hCA I and hCA II, PDB ID:6G3 V and 3PO6, respectively) were obtained from the RCSB database (www.pdb.org). From the experimentally obtained 6G3V (hCA I) and 3PO6 (hCA II) coded structures, the active sites of hCA I and hCA II enzymes were determined and docking procedure was applied to analyze the interactions of **Y6, Y6a,** and **Y6b** ligands at these active sites (Camadan et al. 2022). The grid parameters were selected as 60 × 60 × 60, Å x, y, z dimensions, 0.553 Å space and 20.50, 36.18, 58.96 x, y, z centers for hCA I (PDB ID: 6G3 V) and – 0.36, − 2.19, 11.91 x, y, z centers for hCA II (PDB ID: 3PO6).

The energetically optimal poses of the ligands in the binding site of hCA I and hCA II enzymes, a two-dimensional interaction diagram and a three-dimensional representation of the binding site for **Y6, Y6a,** and **Y6b** ligands are shown in Figs. 3 and 4.

In the molecular docking calculations to the hCA I enzyme, binding energy values of − 5.34, − 5.22, and − 6.45 kcal/mol were obtained for **Y6, Y6a,** and **Y6b** ligands, respectively. According to the binding energy values obtained for **Y6, Y6a,** and **Y6b** ligands, the strongest docking ligand to the hCA I enzyme was the **Y6b** ligand, while the weakest docking ligand was the **Y6a** ligand. It was observed that the **Y6** ligand formed carbon–hydrogen bonds with the Trp5 and VAL62, π-π T-shaped interaction with Trp5, Amide-Pi stacked interaction with Gly63, π-alkyl interactions with His64 and Val62. **Y6a** ligand was observed to have conventional hydrogen bonding with Tyr7 and Hıs243, carbon–hydrogen bonds with Pro240 and Hıs64, π-donor interactions with Tyr7 and Hıs243, π-anion interaction with Asp8, π-π T-shaped interaction with Hıs243, alkyl interaction with Val239, π-alkyl interaction with Hıs243, π-sulfur interaction with Tyr7. **Y6b** ligand was observed to have conventional hydrogen bonding with Hıs67 and Gln92, carbon–hydrogen bond with Thr195, π-donor interaction with Hıs67, π-cation interactions with Hıs200 and Hıs94, π-π T-shaped interactions with His200, His94 and Hıs67, alkyl interactions with Leu198, Val207 and Val143, π-sigma interaction with Leu198, π-alkyl interactions with Ala135, Hıs119, Trp209 and Ala121, π-sulfur interaction with Phe91.

In the molecular docking calculations, binding energy values of **− 5.76, − 5.55,** and **6.28 kcal/mol** were obtained for **Y6, Y6a,** and **Y6b** ligands, respectively. According to the binding energy values obtained for **Y6, Y6a,** and **Y6b** ligands, the strongest docking ligand to the CA II enzyme was the **Y6b** ligand, while the weakest docking ligand was the **Y6a** ligand.

Y6 ligand was observed to dock by carbon–hydrogen bond with Trp5 and Gly63, π-π type interaction with Phe231, amide-π stacked interaction with Tyr7, π-sulfur interaction with Tyr7, alkyl type interaction with Lys170, π-alkyl type interactions with Hıs64 and Hıs62. **Y6a** ligand was observed to make carbon–hydrogen bond with Asn11 and Val242, conventional hydrogen bond Glu239, π-donor hydrogen bonding with Thr7 amino acid, π-sulfur type interactions with His64, Thr7 and Phe231amino acids in the binding site of the target protein and alkyl type interaction with Val242 amino acid. On the other hand, **Y6b** ligand docked to the target protein through π-cation interactions with Hıs94 and Hıs64, π-π type interaction with Hıs 94, π-alkyl interactions with the amino acids Leu198, Pro202, Val135, Val143, Val121 and Ala65 and alkyl interaction with Val135. All these three ligands showed slightly different inhibition activities experimentally, but meaningful differences were not observed through binding energies for them.

Conclusions

As a result, thiophene-based imine and phosphoazomethine compounds (**Y6, Y6a, Y6b**) were synthesized in high yields and the structures of the compounds were confirmed by characterization studies. The synthesis of imine compounds was carried out in a short time of 10 min and in high yield (98%) using the microwave method. The compounds (**Y6, Y6a, Y6b**) were evaluated for their in vitro antioxidant, antimicrobial, enzyme inhibition, and antiproliferative activities and their potential therapeutic effects were revealed. Among the compounds obtained; the highest antioxidant activity (IC_{50}: 5.13 µg/mL (DPPH); 3.98 µg/mL (ABTS) was observed in the **Y6a** compound, the highest inhibitory effect was observed in the **Y6b** compound (IC_{50}: 0.46 µM) for hCA I, and in **Y6a** compound (IC_{50}: 0.56 µM) for hCA II. Antibacterial test results showed that the compounds did not possess antifungal activity but had antibacterial activity against all bacterial strains used (inhibition zones ranged from 8 ± 0.40 to 18 ± 1.30 mm). The results of the antiproliferative assay showed promising results, all three compounds caused a decrease in the growth curve rate in the MCF-7 cell line on a CI basis with an increase in concentration compared to control cells. Compounds **Y6** and **Y6a** (56.58, 51.30 µM) had higher IC_{50} values than cisplatin (40.01 µM) used as the positive control, while compound **Y6b** (43.76 µM) was found to have almost the same effect. These results provided important preliminary information for further detailed

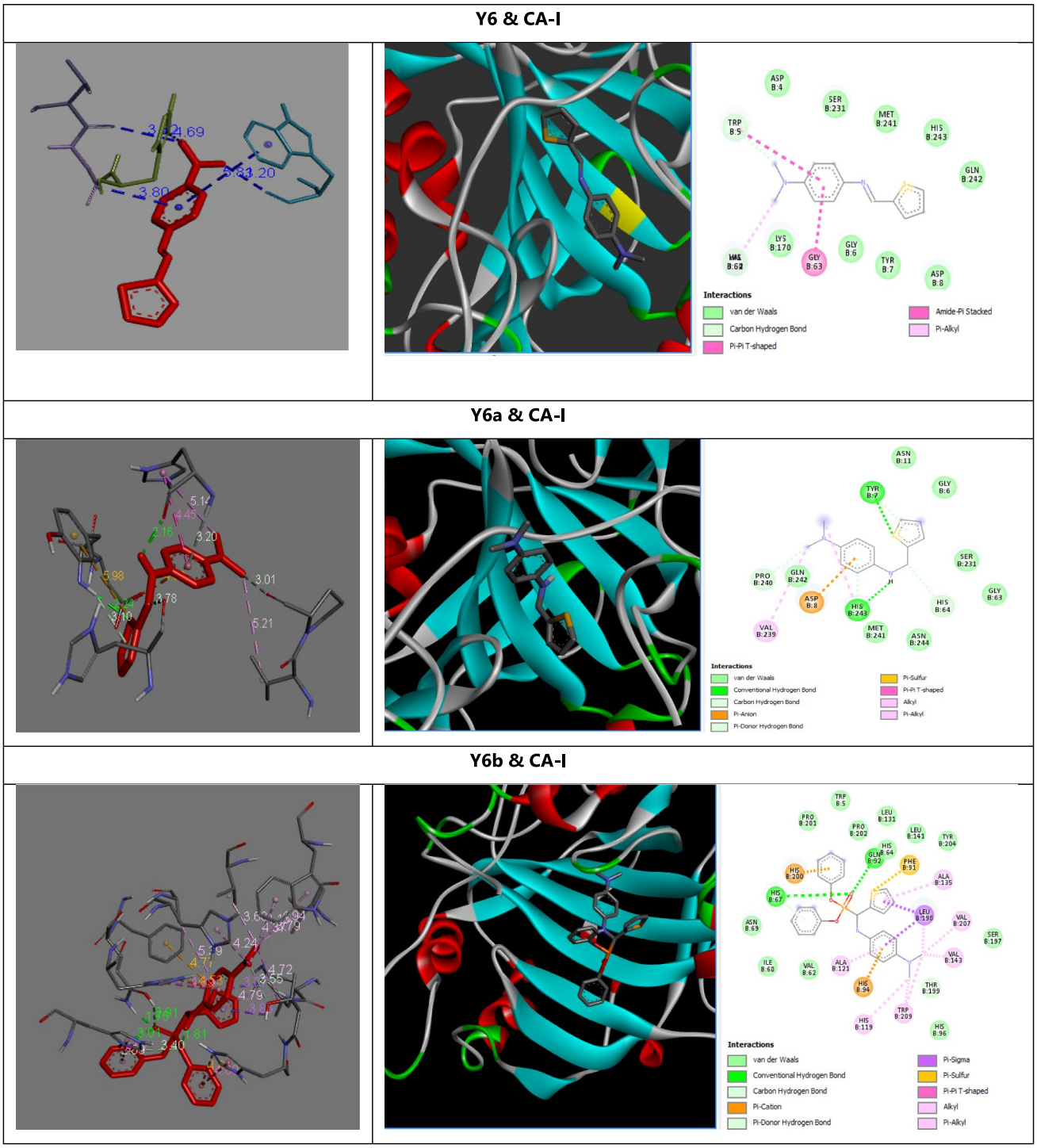

Fig. 3 2-D and 3-D interaction diagrams of hCA I & **Y6-Y6a-Y6b** complexes

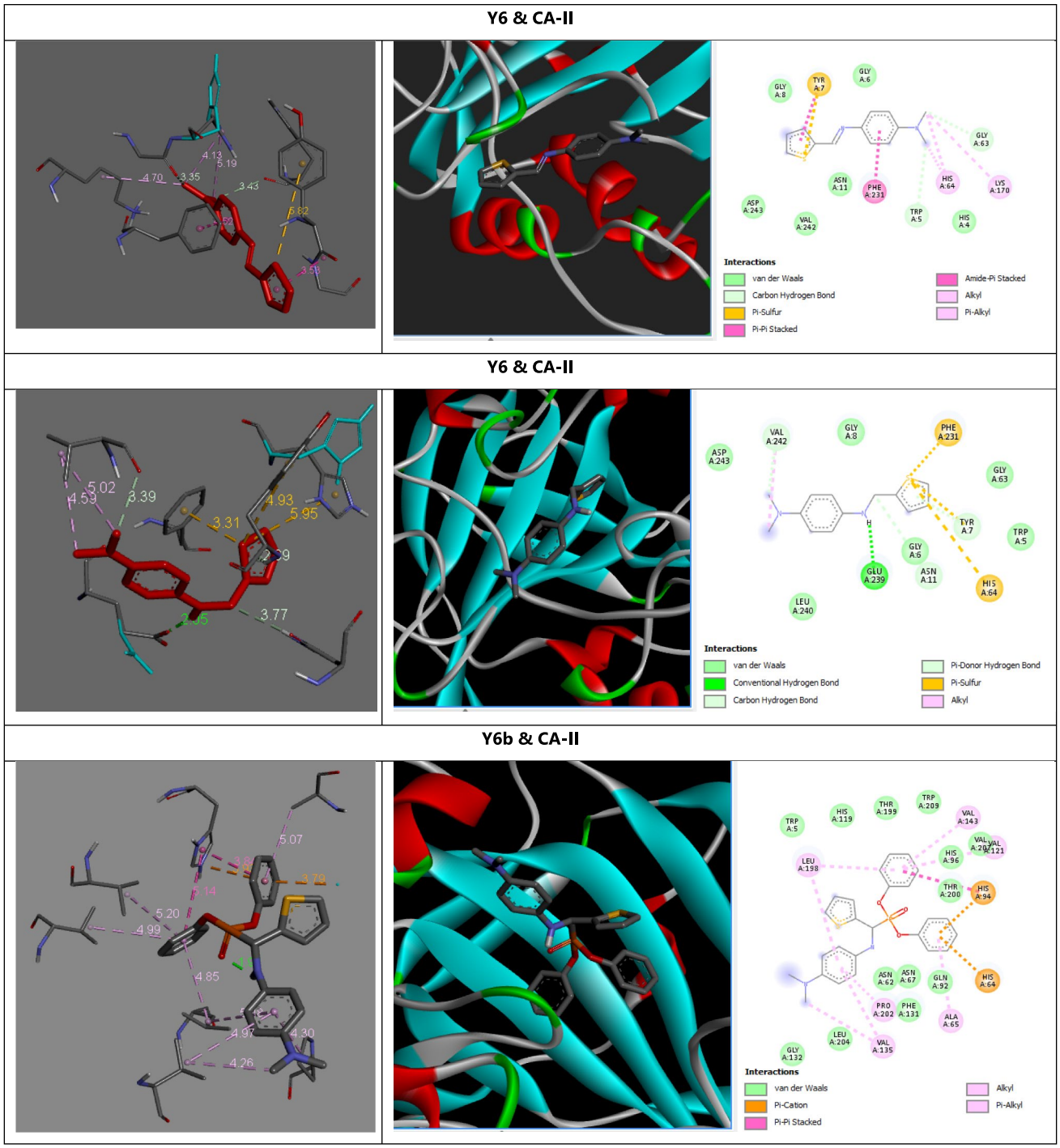

Fig. 4 2-D and 3-D interaction diagrams of hCA I and hCA II & **Y6-Y6a-Y6b** complexes

studies and can be presented as candidates for further biological scientific studies.

Supplementary Information The online version contains supplementary material available at https://doi.org/10.1007/s11696-025-04096-3.

Acknowledgements The authors would like to extend our gratitude to Associate Professor Dr. Zuhal ALIM from the Department of Chemistry, Faculty of Arts and Sciences, Ahi Evran University in Kırşehir, Turkey, for providing us with the hCA I and hCA II isoenzymes used in this study. We would also like to thank Fırat University Scientific Research Projects Coordination Unit for supporting the study (Grant numbers MF.22.01).

Author contributions Synthesis studies were carried out by K.O. and O.G., biological activity studies were performed by K.O., molecular

docking studies were carried out by K.O. and O.G., analysis of the article results was conducted by K.O., M.S.T., H.C. and O.G., and the article was written by K.O.

Declarations

Conflict of interest The authors declare that they have no known competing financial interests or personal relationships that could have appeared to influence the work reported in this paper.

References

Abd Elghany El-Samahy F, Ahmed Ezet Eldeken G, Mostafa ZE, Hassan OF, Elgemeie G (2023) A novel phosphonates synthesized from schiff's base indenoquinoxaline derivatives and its biological activity. ChemistrySelect 8(13):e202300639

Afridi HH, Shoaib M, Al-Joufi FA, Shah SWA, Hussain H, Ullah A, Zahoor M, Mughal EU (2022) Synthesis and investigation of the analgesic potential of enantiomerically pure schiff bases: a mechanistic approach. Molecules 27(16):5206

Aggarwal V, Tuli HS, Varol A, Thakral F, Yerer MB, Sak K, Varol M, Jain A, Khan MA, Sethi G (2019) Role of reactive oxygen species in cancer progression: molecular mechanisms and recent advancements. Biomolecules 9(11):735

Aguilar-Llanos E, Carrera-Pacheco SE, González-Pastor R, Zúñiga-Miranda J, Rodríguez-Pólit C, Romero-Benavides JC, Heredia-Moya J (2022) Synthesis and evaluation of biological activities of schiff base derivatives of 4-aminoantipyrine and cinnamaldehydes. Chem Proc 12(1):43

Ali M, El-Gendy M (2022) Synthesis of new organophosphorus pyrazole derivatives as human myeloblastic leukemia hl60 cytotoxic agents. Egypt J Chem 65(12):27–37

Ali OM, Alotaibi MT, Zaki YH, Amer HH (2022) Design, synthesis, and spectroscopic studies of some new α-aminophosphonate analogues derived from 4-hydroxybenzaldehyde with special reference to anticancer activity. Drug des Dev Ther 16:2589

Ambika S, Manojkumar Y, Arunachalam S, Gowdhami B, Meenakshi Sundaram KK, Solomon RV, Venuvanalingam P, Akbarsha MA, Sundararaman M (2019) Biomolecular interaction, anti-cancer and anti-angiogenic properties of cobalt (iii) schiff base complexes. Sci Rep 9(1):2721

Annan DA, Maishi N, Soga T, Dawood R, Li C, Kikuchi H, Hojo T, Morimoto M, Kitamura T, Alam MT (2019) Carbonic anhydrase 2 (caii) supports tumor blood endothelial cell survival under lactic acidosis in the tumor microenvironment. Cell Commun Signal 17:1–15

Ayaz M, Gündoğdu Ö, Aytaç S, Erdem B, Çiftçi H, Erdogdu Y (2022) Microwave-assisted synthesis, characterizations, antimicrobial activities, and dft studies on some pyridine derived schiff bases. J Mol Struct 1269:133791

Ayobami O, Willrich N, Reuss A, Eckmanns T, Markwart R (2020) The ongoing challenge of vancomycin-resistant enterococcus faecium and enterococcus Faecalis in Europe: an epidemiological analysis of bloodstream infections. Emerg Microbes Infect 9(1):1180–1193

Aytac S, Gundogdu O, Bingol Z, Gulcin İ (2023) Synthesis of schiff bases containing phenol rings and investigation of their antioxidant capacity, anticholinesterase, butyrylcholinesterase, and carbonic anhydrase inhibition properties. Pharmaceutics 15(3):779

Aytaç S (2021) Schiff bazı bileşiklerinin çevreci bir yöntemle yeniden sentezi. J Inst Sci Technol 11(4):2979–2991

Berkow EL, Lockhart SR, Ostrosky-Zeichner L (2020) Antifungal susceptibility testing: current approaches. Clin Microbiol Rev. https://doi.org/10.1128/cmr.00069-19

Blois MS (1958) Antioxidant determinations by the use of a stable free radical. Nature 181(4617):1199–1200

Buldurun K, Turan N, Aras A, Mantarcı A, Turkan F, Bursal E (2019) Spectroscopic and structural characterization, enzyme inhibitions, and antioxidant effects of new ru (ii) and ni (ii) complexes of schiff base. Chem Biodivers 16(8):e1900243

Camadan Y, Çiçek B, Adem Ş, Çalişir Ü, Akkemik E (2022) Investigation of in vitro and in silico effects of some novel carbazole schiff bases on human carbonic anhydrase isoforms i and ii. J Biomol Struct Dyn 40(15):6965–6973

Cauli O (2021) Oxidative stress and cognitive alterations induced by cancer chemotherapy drugs: a scoping review. Antioxidants 10(7):1116

Chen F-F, He X-F, Zhu X-X, Zhang Z, Shen X-Y, Chen Q, Xu J-H, Turner NJ, Zheng G-W (2023) Discovery of an imine reductase for reductive amination of carbonyl compounds with sterically challenging amines. J Am Chem Soc 145(7):4015–4025

Da Silva CM, da Silva DL, Modolo LV, Alves RB, de Resende MA, Martins CV, de Fátima Â (2011) Schiff bases: a short review of their antimicrobial activities. J Adv Res 2(1):1–8

Durmaz L, Erturk A, Akyüz M, Polat KL, Uc EM, Bingol Z, Saglamtas R, Alwasel S, Gulcin İ (2022) Screening of carbonic anhydrase, acetylcholinesterase, butyrylcholinesterase, and α-glycosidase enzyme inhibition effects and antioxidant activity of coumestrol. Molecules 27(10):3091

Eleamen GR, Costa SCD, Lima-Neto RG, Neves RP, Rolim LA, Rolim-Neto PJ, Moura RO, Aquino TMD, Bento ES, Scotti MT (2017) Improvement of solubility and antifungal activity of a new aminothiophene derivative by complexation with 2-hydroxypropyl-β-cyclodextrin. J Braz Chem Soc 28:116–125

Finkbeiner P, Hehn JRP, Gnamm C (2020) Phosphine oxides from a medicinal chemist's perspective: physicochemical and in vitro parameters relevant for drug discovery. J Med Chem 63(13):7081–7107

Francioso A, Conrado AB, Mosca L, Fontana M (2020) Chemistry and biochemistry of sulfur natural compounds: key intermediates of metabolism and redox biology. Oxidative Med Cell Longevity 2020:8294158

Gholivand K, Koupaei MHH, Mohammadpanah F, Roohzadeh R, Fallah N, Pooyan M, Satari M, Pirastehfar F (2022) A novel phospho triazine compound serving as an anticancer and antibacterial agent: an experimental-computational investigation. J Mol Struct 1263:133024

Gülçin İ, Trofimov B, Kaya R, Taslimi P, Sobenina L, Schmidt E, Petrova O, Malysheva S, Gusarova N, Farzaliyev V (2020) Synthesis of nitrogen, phosphorus, selenium and sulfur-containing heterocyclic compounds–determination of their carbonic anhydrase, acetylcholinesterase, butyrylcholinesterase and α-glycosidase inhibition properties. Bioorg Chem 103:104171

Haapasalo J, Nordfors K, Haapasalo H, Parkkila S (2020) The expression of carbonic anhydrases ii, ix and xii in brain tumors. Cancers 12(7):1723

Huyut Z, Beydemir Ş, Gülçin İ (2016) Inhibitory effects of some phenolic compounds on the activities of carbonic anhydrase: from in vivo to ex vivo. J Enzyme Inhib Med Chem 31(6):1234–1240

Ignatovich ZV, Kadutskii A, Koroleva E, Baranovskii A, Gusak K (2009) Reductive transformations of schiff bases in the synthesis of functionally substituted heteroaromatic amines. Russ J Org Chem 45:1070–1078

Iwanejko J, Wojaczyńska E, Turlej E, Maciejewska M, Wietrzyk J (2020) Octahydroquinoxalin-2 (1 h)-one-based aminophosphonic acids and their derivatives—biological activity towards cancer cells. Materials 13(10):2393

Iwanejko J, Samadaei M, Pinter M, Senfter D, Madlener S, Kochel A, Rohr-Udilova N, Wojaczyńska E (2021) Cytotoxic activity of

piperazin-2-one-based structures: cyclic imines, lactams, aminophosphonates, and their derivatives. Materials 14(9):2138
Khan A (2019) Immunoliposomes-mediated small interfering rna therapy: a novel approach for the treatment of cancer. Int J Health Sci 13(2):1
Köksal Z, Alım Z, Bayrak S, Gülçin İ, Özdemir H (2019) Investigation of the effects of some sulfonamides on acetylcholinesterase and carbonic anhydrase enzymes. J Biochem Mol Toxicol 33(5):e22300
Kundu S, Pramanik AK, Mondal AS, Mondal TK (2016) Ni (ii) and pd (ii) complexes with new n, o donor thiophene appended schiff base ligand: synthesis, electrochemistry, x-ray structure and dft calculation. J Mol Struct 1116:1–8
Lewis I, James S (2022) Performance standards for antimicrobial susceptibility testing. Clinical and laboratory standards institute
Liu Z, Li H, Qi Y, Zhu Z, Huang D, Zhang K, Pan J, Wen L, Zou Z (2021) Cinnamomum camphora leaves as a source of proanthocyanidins separated using microwave-assisted extraction method and evaluation of their antioxidant activity in vitro. Arab J Chem 14(9):103328
Marchi RC, Campos IA, Santana VT, Carlos RM (2022) Chemical implications and considerations on techniques used to assess the in vitro antioxidant activity of coordination compounds. Coord Chem Rev 451:214275
Mboge MY, Mahon BP, McKenna R, Frost SC (2018) Carbonic anhydrases: role in ph control and cancer. Metabolites 8(1):19
Nasser A, Migahed M, EL Basiony N, Abd-El-Bary H, Mohamed TA (2023) Raman and infrared spectral analysis, normal coordinate analysis, dft calculations of novel schiff base containing di-imine moieties. Egypt J Chem 66(9):271–291
Nguyen DT, Le TH, Bui TTT (2013) Antioxidant activities of thiosemicarbazones from substituted benzaldehydes and n-(tetra-o-acetyl-β-d-galactopyranosyl) thiosemicarbazide. Eur J Med Chem 60:199–207
Nocentini A, Gratteri P, Supuran CT (2019) Phosphorus versus sulfur: discovery of benzenephosphonamidates as versatile sulfonamide-mimic chemotypes acting as carbonic anhydrase inhibitors. Chem A Eur J 25(5):1188–1192
Oboňová B, Habala L, Litecká M, Herich P, Bilková A, Bilka F, Horváth B (2023) Antimicrobially active zn (ii) complexes of reduced schiff bases derived from cyclohexane-1, 2-diamine and fluorinated benzaldehydes—synthesis, crystal structure and bioactivity. Life 13(7):1516
Pathania S, Narang RK, Rawal RK (2019) Role of sulphur-heterocycles in medicinal chemistry: an update. Eur J Med Chem 180:486–508
Puchtler H, Meloan S (1981) On schiff's bases and aldehyde-fuchsin: a review from h. Schiff to Rd Lillie. Histochemistry 72(3):321–332
Re R, Pellegrini N, Proteggente A, Pannala A, Yang M, Rice-Evans C (1999) Antioxidant activity applying an improved abts radical cation decolorization assay. Free Radical Biol Med 26(9–10):1231–1237
Rostamizadeh M, Maghsoodlou MT, Hazeri N, Habibi-khorassani SM, Keishams L (2011) A novel and efficient synthesis of α-aminophosphonates by use of triphenyl phosphite in acetic acid media. Phosphorus Sulfur Silicon Relat Elem 186(2):334–337
Roy S, Trinchieri G (2017) Microbiota: a key orchestrator of cancer therapy. Nat Rev Cancer 17(5):271–285
Satapathy AK, Behera SK, Yadav A, Mahour LN, Yelamaggad C, Sandhya K, Sahoo B (2019) Tuning the fluorescence behavior of liquid crystal molecules containing schiff-base: effect of solvent polarity. J Lumin 210:371–375
Savcı A, Buldurun K, Alkış ME, Alan Y, Turan N (2022) Synthesis, characterization, antioxidant and anticancer activities of a new schiff base and its m (ii) complexes derived from 5-fluorouracil. Med Oncol 39(11):172
Shams-White MM, Romaguera D, Mitrou P, Reedy J, Bender A, Brockton NT (2020) Further guidance in implementing the standardized 2018 world cancer research fund/american institute for cancer research (wcrf/aicr) score. Cancer Epidemiol Biomark Prev 29(5):889–894
Shanty AA, Philip JE, Sneha EJ, Kurup MRP, Balachandran S, Mohanan PV (2017) Synthesis, characterization and biological studies of schiff bases derived from heterocyclic moiety. Bioorg Chem 70:67–73
Sobati M, Abdoli M, Bonardi A, Gratteri P, Supuran CT, Žalubovskis R (2023) Inhibition profiles of some novel sulfonamide-incorporated α-aminophosphonates on human carbonic anhydrases. ACS Med Chem Lett 14(8):1067–1072
Spagnolo AM, Sartini M, Cristina ML (2021) Pseudomonas aeruginosa in the healthcare facility setting. Rev Res Med Microbiol 32(3):169–175
Tlidjane H, Chafai N, Chafaa S, Bensouici C, Benbouguerra K (2022) New thiophene-derived α-aminophosphonic acids: Synthesis under microwave irradiations, antioxidant and antifungal activities, dft investigations and sars-cov-2 main protease inhibition. J Mol Struct 1250:131853
Tuli HS, Kaur J, Vashishth K, Sak K, Sharma U, Choudhary R, Behl T, Singh T, Sharma S, Saini AK (2023) Molecular mechanisms behind ros regulation in cancer: a balancing act between augmented tumorigenesis and cell apoptosis. Arch Toxicol 97(1):103–120
Türker Şener L, Albeni̇z G, Dïnç BR, Albeni̇z I (2017) Icelligence real-time cell analysis system for examining the cytotoxicity of drugs to cancer cell lines. Exp Ther Med 14(3):1866–1870
Uhlen M, Zhang C, Lee S, Sjöstedt E, Fagerberg L, Bidkhori G, Benfeitas R, Arif M, Liu Z, Edfors F (2017) A pathology atlas of the human cancer transcriptome. Science 357(6352):eaan2507
Ullah AAAM (2020) Synthesis and evaluation of novel heterocyclic compounds as anticancer agents. University of Salford (United Kingdom)
Uluçam G, Okan ŞE, Aktaş Ş, Yentürk B (2021) New schiff-base ligands containing thiophene terminals: synthesis, characterization and biological activities. J Mol Struct 1230:129941
Venkateswarlu K, Kumar MP, Rambabu A, Vamsikrishna N, Daravath S, Rangan K (2018) Crystal structure, DNA binding, cleavage, antioxidant and antibacterial studies of cu (ii), ni (ii) and co (iii) complexes with 2-((furan-2-yl) methylimino) methyl)-6-ethoxyphenol schiff base. J Mol Struct 1160:198–207
Verpoorte JA, Mehta S, Edsall JT (1967) Esterase activities of human carbonic anhydrases b and c. J Biol Chem 242(18):4221–4229
Vukovic N, Sukdolak S, Solujic S, Niciforovic N (2010) Substituted imino and amino derivatives of 4-hydroxycoumarins as novel antioxidant, antibacterial and antifungal agents: Synthesis and in vitro assessments. Food Chem 120(4):1011–1018
Winum JY, Innocenti A, Gagnard V, Montero JL, Scozzafava A, Vullo D, Supuran CT (2005) Carbonic anhydrase inhibitors. Interaction of isozymes i, ii, iv, v, and ix with organic phosphates and phosphonates. Bioorgan Med Chem Lett 15(6):1683–1686
Ye M-Y, Yao G-Y, Pan Y-M, Liao Z-X, Zhang Y, Wang H-S (2014) Synthesis and antitumor activities of novel α-aminophosphonate derivatives containing an alizarin moiety. Eur J Med Chem 83:116–128

Yigit M, Celepci D, Taslimi P, Yigit B, Cetinkaya E, Ozdemir I, Aygun M, Gulcin I (2022). Selenourea and thiourea derivatives of chiral and achiral enetetramines

Yiğit B, Yiğit M, Taslimi P, Gök Y, Gülçin İ (2018) Schiff bases and their amines: synthesis and discovery of carbonic anhydrase and acetylcholinesterase enzymes inhibitors. Arch Pharm 351(9):1800146

Zareei S, Mohammadi-Khanaposhtani M, Adib M, Mahdavi M, Taslimi P (2023) Sulfonamide-phosphonate hybrids as new carbonic anhydrase inhibitors: in vitro enzymatic inhibition, molecular modeling, and admet prediction. J Mol Struct 1271:134114

Zheng Y, Xu B, Zhao Y, Gu H, Li C, Wang Y, Chang X (2015) Ca1 contributes to microcalcification and tumourigenesis in breast cancer. BMC Cancer 15:1–15